Investigation and Modeling of Large Barkhausen Jumps Dynamics in Low-Power Fluxgate Magnetometers

Eyal Weiss, Roger Alimi, Amir Ivry, and Elad Fisher

***Abstract*— Large Barkhausen jumps occur in low-power fluxgates output and seriously affect the signal fidelity and therefore the magnetometer functionality. In this paper, we investigate the occurrence of DC jumps in two types of fluxgates, parallel and orthogonal. We present a new model for the jumps phenomenon. This model is based on the reversal dynamics of magnetic domains in the core metallurgical super-structures. We expand the model to explain how and why the jumps subside in time. We show that although the jumps rate decays exponentially in time, the process never completely stops. The understanding of DC jumps dynamics may be utilized in research and development of low-power magnetic sensors. It may be used to characterize and standardize the quality of magnetic sensors cores and used to screen faulty cores that exhibit exceptionally high jump rate that may affect signal fidelity. Mitigating the jumps in both parallel and orthogonal low-power fluxgates is crucial for low-noise magnetic measurement systems.**

***Index Terms*— Magnetometers, low power, Barkhausen noise, magnetic noise, DC jumps, detection algorithm, signal fidelity.**

I. Introduction

FLUXGATE magnetometers are induction sensors utilizing a ferromagnetic core which is saturated periodically to modulate the measured magnetic field [1]. There are two types of fluxgates; A parallel fluxgate [2] where the core excitation magnetic field is parallel to the measured field and an orthogonal fluxgate [3] where the excitation field is orthogonal to it. Parallel fluxgates cores are excited by a bipolar magnetic field and orthogonal fluxgates [4] are best modulated by a unipolar field [5].

Fluxgates are commonly used in large sensor arrays for surveillance applications [6]. This is because they are sensitive, small, and are relatively inexpensive. When employing a sensor array it is essential to maintain low power consumption. This is true both in wireless and wired arrays. Power consumption reduction in fluxgates were achieved in both orthogonal [7]–[9] and in parallel fluxgates [10]. Unfortunately, it is well known that the noise level generally increases when decreasing the fluxgate excitation power [11].

Unfortunately, decreasing the power consumption in fluxgates comes at a cost. The power consumption reduction is mostly achieved by decreasing the core excitation field [12]. As a result, the fluxgate core does not undergo deep and uniform saturation [13] and the magnetization of the core is inhomogeneous. The weak magnetic saturation results in smaller rotation forces applied to the magnetic domains compared to conventional fluxgates [14]. As a result, low power fluxgates tend to suffer from *DC* jumps in their output. This phenomenon does not occur in sensors that do not employ a magnetic core such as Lorentz force magnetometer [15], [16], Hall effect [17], [18], and planar Hall effect sensors [19]. However, conventionally, core-less sensors have much lower sensitivity. An example of fluxgate output jump is presented in Fig. 1.

Conventionally, noise spectrum is evaluated by performing noise measurement in a shielded environment for a long period of time. In this scenario, a *DC* jump embedded in the measurement typically does not significantly affect the noise power spectrum density figure because of its singularity. The sensor noise is evaluated by long-term averaging of the spectrum, so that the results are stable and include jumps, and averaging with reasonable overlap can be used to describe classical noise. Nevertheless, the *DC* jumps statistics complete the characterization of the sensors' performance. As a result, a low power sensor may present deceptively low spectral noise, but due to random jumps will have poor signal fidelity. This is important because magnetic surveillance systems operate in the time domain [6], [20] and are therefore sensitive to signal fidelity.

A physical description of jumps in the output of low power fluxgates is first introduced by Weiss and Alimi [21]. In this work, we present a physical model for the jumps in low power fluxgates. We propose that because of the low saturation excitation field, some magnetic domains are temporarily "stuck" in one magnetization direction. They are stuck on metallurgical imperfections in the lattice [13], while the rest of the core domains continue in periodical rotations.

The "stuck" domains disturb the effective permeability of the core, which is translated to a rapid change in fluxgate sensitivity. The occurrence of this phenomenon is stochastic and the unstable domain may snap back and forth to alignment at random time and cause a sudden offset in sensitivity [22], [23] which in turn creates a voltage jump in the output of the fluxgate [12]. This *DC* jump (Fig. 1) is a major source of internal magnetic noise.

In this work, we research the phenomena of *DC* jumps in low power fluxgates. We statistically investigate the dynamics of the jumps by employing an algorithm able to efficiently

Manuscript received August 28, 2018; revised October 28, 2018 and December 5, 2018; accepted December 5, 2018. Date of publication December 10, 2018; date of current version February 15, 2019. The associate editor coordinating the review of this paper and approving it for publication was Prof. Sheng-Shian Li. *(Corresponding author: E. Weiss.)*

The authors are with the Technology Division, Soreq NRC, Yavne 81800, Israel (e-mail: eyal_we@soreq.gov.il).

Digital Object Identifier 10.1109/JSEN.2018.2885779

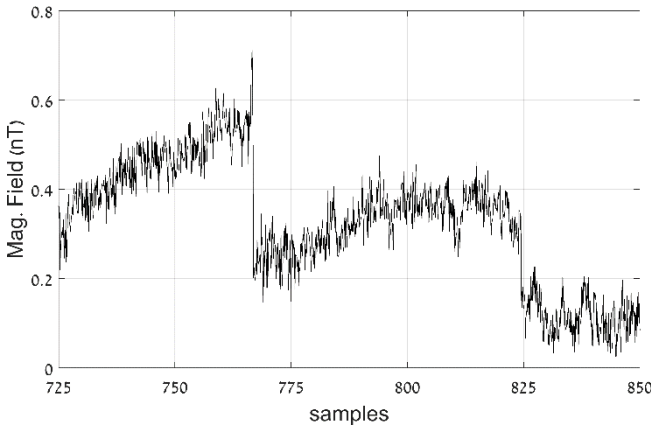

Fig. 1. An example of magnetic noise in low power parallel fluxgate magnetometer with a DC jump. The DC jump is the negative steps visible at samples ∼760 and ∼825.

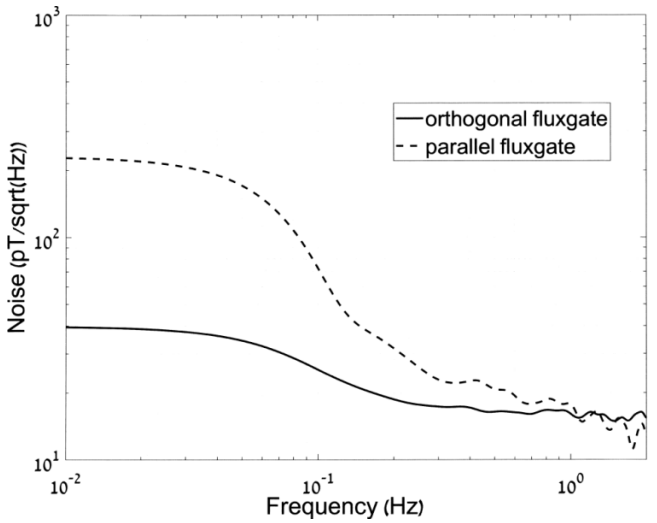

Fig. 2. Measured noise of the digital orthogonal and parallel fluxgates. The noise level at 1Hz is almost identical while the flicker noise of the orthogonal fluxgate is significantly lower. The measurements were made when no *DC* jumps occurred.

detect the jumps based on convolution with a customized kernel. We then present an established experimentally physical model for the *DC* jumps based on an expansion of the Landau Lifshitz Gilbert (*LLG*) equation and an expansion to include the core excitation dynamics. This model can be used to better design fluxgates and to improve screening of sensors in a production assembly line.

II. Experimental

A. DC Jumps Dynamics Measurement

The *DC* jump rate change over time from power-up. Understanding the long time scale dynamics of the *DC* jumps gives insight to its physical source.

The *DC* jumps of an orthogonal fluxgate was measured inside a 5-shells magnetic shield using a 3-axial orthogonal fluxgate we have constructed as described in [7] with an additional feedback coil. The parallel and orthogonal magnetometers we use are commercial of the shelf Bartington Mag648 and SNRC-BGU BW3 respectively. Their schematic interface circuit systems and corresponding testing circuit are described in [1] and [24]. The Co-based amorphous wire core is excited using *AC* current of 32 mA and *DC* bias of 34 mA. The analog sensor sensitivity is ∼2 mV/μT and the typical output noise is <20 pT/$\sqrt{}$Hz at 1 Hz as measured with no *DC* jumps and presented in Fig. 2. The fluxgate excitation field is performed by driving *AC* current with a *DC* bias through the core, thus the field in the core does not reverse its direction. Where a large enough offset in the excitation field is applied [3] there are less *DC* jumps in the fluxgate output. However, increasing the *DC* excitation bias decreases the fluxgate sensitivity, increases its' magnetic noise as well as its' power consumption. The *DC* jumps magnitude was in the order of 1-nT.

The *DC* jumps dynamics on a parallel 3-axial fluxgate with a bipolar excitation was investigated using data from a large batch of commercial Bartington Mag648 magnetometers [25]. The sensor sensitivity is 50 mV/μT and the typical output noise is <20 pT/$\sqrt{}$Hz at 1 Hz as measured at a period excluding the *DC* jumps and presented in Fig. 2. To evaluate the *DC* jumps occurrence we followed three experimental procedures: (1) short time-scale (40 minutes), (2) long time scale (from to 20 to 48 hours) and (3) short time scale after 48 hours of power soak. The third procedure was used in order to allow efficient screening of sensors after 48 hours of operation without actually performing the measurements throughout.

We have also measured the *DC* jumps rate while operating in different temperatures. We have tested 6 orthogonal fluxgates and 6 parallel fluxgates using experimental procedure (1) at −20, 25, 50 °C. We placed the sensor inside 3-shells magnetic shield with an internal temperature monitored chamber and measured the *DC* jumps. We observed no significant temperature dependency.

B. Short Time Scale Jumps

The sensor was powered for 30 minutes of warm up time. Then the sensor output was recorded for the sequential 40 minutes. A jump algorithm detection was then applied to list the jumps. The first 40 minutes were divided to 8 bins of 5 minutes each. The number of jumps in each time bin was calculated and plotted (Fig. 3).

For every sensor, the jumps' dynamics is different. This is because the jumps are a stochastic phenomenon relating to a specific magnetic core. Fig. 3 depicts three examples of jumps' dynamics we measured in different sensors. The (+) markers curve is an example of a sensor with small amount of jumps that subside within 15 minutes after the warm up time. The average behavior of *DC* jumps for a population of 600 sensors axes is presented in Fig.3 by the (□) markers, it appears to relax after 25 minutes. The (◊) markers curve in Fig. 3 is an example of a sensor that does not appear to relax within the 40 minutes of the measurement. This sensor should be screened by this test as a "jumpy" sensor.

As expected the average gradually decreases with time indicating an intrinsic natural relaxation process. This decrease can be best fitted by a parabola with a moderate negative slope.

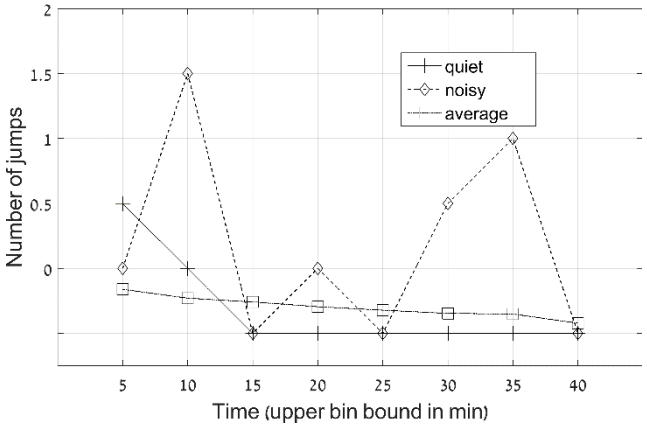

Fig. 3. *DC* jumps time dependency after warm-up in a quiet (+), average (□) and noisy (◊) sensor respectively.

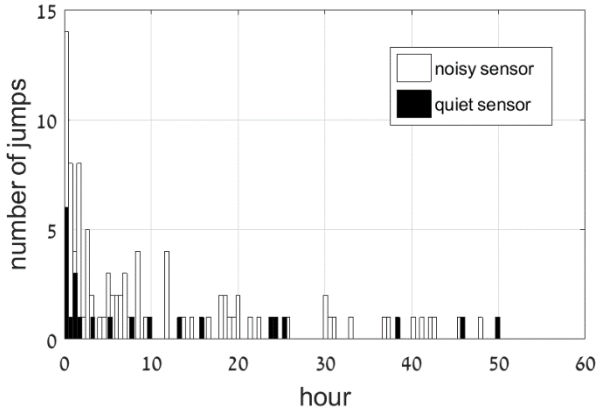

Fig. 4. *DC* jumps time distribution during 48 hours tests for a quiet (a) and noisy (b) sensors.

C. Long Time Scale Jumps

Some 8 parallel low power tri-axial sensors (24 axes) were measured for a time period of 48 hours (Fig. 4). An example of a stable sensor is presented by the black markers in Fig. 4 where the jumps subside quickly while the white markers present the jumps' dynamics for a "jumpy" sensor. Even stable sensors exhibit erratic jumps after long time relaxation.

The sensors were operated for 48 hours in the natural magnetic field, then disconnected, and immediately reconnected in a zero-gauss chamber for the jumps test. One can clearly see in Fig. 5 a significant decrease in the average number of jumps after the 48 hours soak.

The long-time dynamics can be estimated by computing the average number of jumps over time. The result is shown in Fig. 6 together with an exponential fit. Only times larger than 3 hours have been considered to separate small from large time scales.

Furthermore, we have observed that while jumps subside in time during continuous operation, after powering down and powering up of the fluxgate the jumps initiate. The experimental results clearly show that the jumps are a stochastic phenomenon that can be described using statistical analysis. For a specific fluxgate sensor, the occurrence of the jumps decays with time during continuous operation.

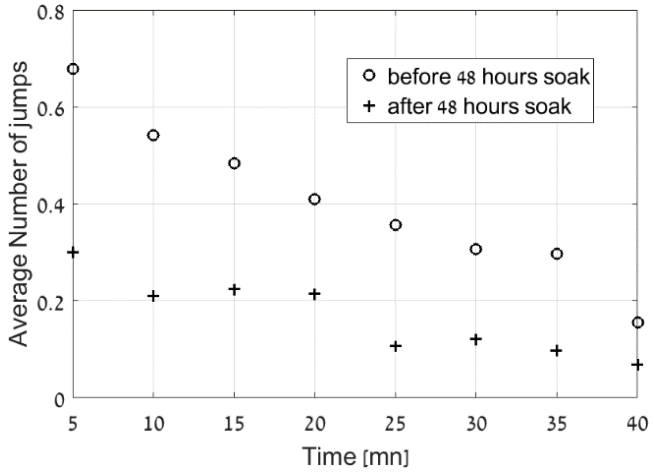

Fig. 5. *DC* jumps time average behavior before and after 48 hours' soak.

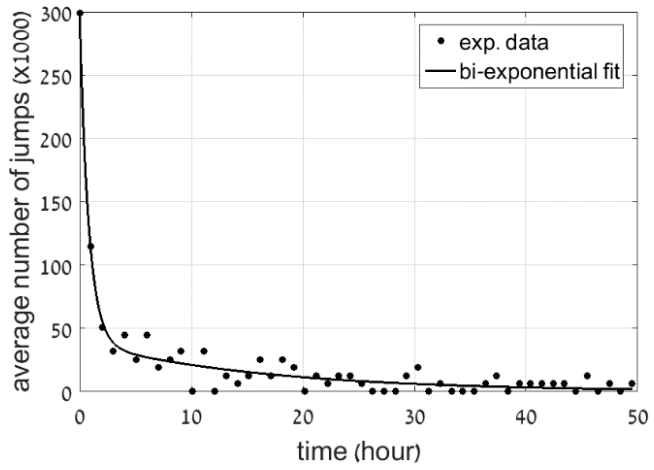

Fig. 6. Average number of *DC* jumps time during 48 hours recording.

The statistical decay is described by a bi-exponential fit according to:

$$y = ae^{-bx} + ce^{-dx}, \tag{1}$$

where a = 260.7, b = 1.239, c = 39.14 and d = 0.062.

Nevertheless, some erratic jumps take place even after 48 hours of operation only at a slower and unpredictable rate. The exact time when the jump will take place is random as far as this work can conclude. However, some sensors repeatedly tend to have more jumps as compared to other ones. This suggests that the amount of jumps is inherent to each individual sensor.

III. Large Barkhausen Jumps Model

DC jumps are characterized by a random and sudden change in fluxgate output voltage (Fig. 1), the occurrence of which subside in time. We present a model for the *DC* jump phenomena in the cores of fluxgates in two types of fluxgates, which differ by the way their core is being excited. We then expand the model to explain why the jumps subside in time.

A. Model of Large Barkhausen Jumps in Parallel Fluxgates

Parallel fluxgates are operated by employing a bi-polar excitation magnetic field to the core. The magnetic domains

in the core, are rotated periodically by the reversals of the excitation magnetic field direction.

In conventional fluxgates the excitation field required to drive the core to deep saturation is of approximately 20 kA/m [26]. In low power fluxgates, the excitation field is an order of magnitude smaller, and as a result, the magnetization uniformity is lower. The magnetization non-uniformity is further enhanced by the demagnetizing effect caused by the rod structure of the core [27], and by super-structures in the core, such as material casting imperfections, random metallurgical grains, dislocations, and surface roughness [28].

An additional source of magnetization inhomogeneity is the internal stress imprinted during the wire casting. The stress is inhomogeneous across the core and as a result the domains switching field is inhomogeneous as well [29].

We suggest that the core magnetization inhomogeneity caused by the mechanisms described is the source of the jumps (see Fig. 7).

This is because the magnetization reversals mechanism in bi-polar excitation fluxgates consist of domain walls motion, coherent domain rotations, and nucleation of domains [30]. Any super-structure or inhomogeneity in the core is a source of inhibition to the smooth rotations of the domains [12]. The domain re-organization during excitation may be localized in the core by the source of rotation inhibition, where a part of the domain wall or an entire domain may jump to an adjacent stable position [12]. This domain snap, results in a jump in the fluxgate sensitivity.

B. Model of DC Jumps in Orthogonal Fluxgates

Orthogonal fluxgates are operated by employing a unipolar excitation magnetic field to the core by driving current through it. The excitation direction is circular across the wire core. The coherent rotation of magnetization [5] is exploited in a fundamental-mode orthogonal fluxgate [17], [18]. In this method the excitation field never reaches zero as the entire excitation cycle is unipolar with a *DC* bias.

However, the magnetization across the core in orthogonal fluxgates is inherently non-uniform [13]. In this excitation scheme, the excitation magnetic field increases from the inner core to the periphery. As a result, the periphery of the core is driven to saturation by the current while the inner shells of the wire core magnetization level is weaker.

In the neutral center of the wire, the domains are free to nucleate and shift. The natural magnetization direction of the inner core is axial because of its high effective permeability due to its length to diameter ratio [27]. As a result, there is a gradient of magnetization level across the core in both amplitude and direction. An unstable "spring onion" like boundary layer of magnetic domains separates between the two domain regimes [13]. When this unstable layer transforms it causes magnetic noise in the core.

IV. DC Jumps Dynamic Model

A. Dynamics of a Single DC Jump

In this section, we analyze the *DC* jumps evolution during the fluxgate operation. As described earlier, *DC* jumps are caused by movement of domains or domain walls that got "stuck" in the core lattice. In Section II we present the measured dynamics of the *DC* jumps. Nevertheless, the reason why this phenomenon subsides in time remains unexplained. Experimental visualization of the *DC* jumps may be performed by employing Magneto-Optical Kerr Effect (NanoMOKE), which, in certain conditions, allows the observation of the magnetic domains structure by MOKE microscopy, but is out of the scope of this work.

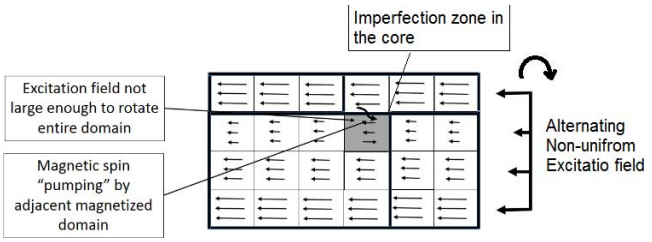

Fig. 7. Illustration of the excitation of a magnetic core. The shaded domain does not align to the external excitation field because it is inhibited by an imperfection in the core.

One possible explanation [12] is that the permanent re-magnetization of the domains lead to domain walls "smoothening" after numerous conjoint frictions. During excitation, there may be conditions for self-homogenization due to the rise of temperature, which supplies the necessary energy for liquidation of the material structural impurities. However, according to this explanation the lattice becomes plastically "homogenous" after some "self-healing" time. Nevertheless, we have observed that while jumps subside in time during continuous operation, after powering down and powering up of the fluxgate the jumps re-initiate. We can therefore conclude that the self-homogenization of the core is not permanent.

Another possible explanation is that the self-homogenization of fluxgates cores is a dynamic process where zones in the core with different magnetization levels interact. A model for the core "self-homogenization" was presented in [13] for an orthogonal fluxgate operating in duty cycle. In duty cycle operation of orthogonal fluxgates, idle intervals are introduced between excitation cycles. The idle intervals leave enough time for "self-homogenization" of the magnetization gradient in the core.

Similarly, in parallel fluxgate cores, the "stuck" zones near imperfections are not in equilibrium because they share boundary with other domains that are pumping out its spin energy in every excitation cycle [33] (see Fig. 7). When, in time, enough energy is pumped by the spin gradient to equalize the coercive energy required by the domain, it will relax its coercive energy and transform. The relaxation occurs in a "snap" and is a stochastic process, which involves rapid motion of the domain walls.

At the spin level, the magnetization process is conventionally described by the Landau-Lifshitz-Gilbert Equation (*LLG*) [27]:

$$\frac{\partial \boldsymbol{M}}{\partial t} = \gamma\, \boldsymbol{M} \times \boldsymbol{H}^{eff} - C\left(\boldsymbol{M} \times \frac{\partial \boldsymbol{M}}{\partial t}\right), \tag{2}$$

where $\boldsymbol{M}$ is the magnetic moment, $\boldsymbol{H^{eff}}$ is the effective magnetic field, γ is a known gyromagnetic constant ratio, and C is a phenomenological constant. The first term in the right side of Eq. (2) describes the non-dissipative precession motion of the magnetization. The second term is a modification of the dissipative damping term $\boldsymbol{M} \times \left(\boldsymbol{M} \times \boldsymbol{H^{eff}}\right)$ already present in the original Landau Lifshitz (*LL*) formulation [34].

The reformulation of the *LLG* dynamics due to the presence of impurities within an "ideal" magnetic domains structure has been investigated by Squire *et al.* [29]. The author suggests that a defect in the magnetic amorphous core may exert internal friction on the domain wall, which can halt their motion. As a result, the domain wall may be pinned. Unpinning it requires larger effective magnetic field, which may not be available at any moment. The additional unpinning energy may be provided by introducing small recurring dissipative process. Such a mechanism would account for the *Barkhausen effect*.

In [35], it was proposed to replace the effective magnetic field $\boldsymbol{H^{eff}}$ in Eq. (2) by the a modified $\boldsymbol{H^{eff}_{mod}}$ which comprises a formulation of the unpinning mechanism;

$$\boldsymbol{H}^{eff}_{mod} = \boldsymbol{H}^{eff} - \eta\alpha\left[\frac{\partial \boldsymbol{M}}{\partial t}\right], \tag{3}$$

where α is a function defined by the multi-valued relation $\alpha[\boldsymbol{u}] \equiv \frac{\boldsymbol{u}}{|\boldsymbol{u}|}$ if $\boldsymbol{u} \neq 0$, while $\alpha[0]$ is defined to be any vector with modulus not larger than 1.

When the argument of α, $\frac{\partial \boldsymbol{M}}{\partial t} = 0$ the value of $\alpha\left[\frac{\partial \boldsymbol{M}}{\partial t}\right]$ is selected by the specific process, which is uniquely determined despite the fact that α is multivalued; η is a positive coefficient which accounts for the average distribution of the impurities in the material.

If $\left|\boldsymbol{H}^{eff}_{mod}\right| > \eta$ the domain magnetization can change and the wall is free to move.

We suggest that the additional required energy will be eventually gained as the cycling excitation process goes on, although this occurs on a much longer time scale than the common dissipative effect. In every excitation cycle, the magnetization direction rotates. The rotation drives the core to deep saturation where the domains are in an extremity configuration and then relaxes it. This cycling magnetization rotation is accompanied by hysteresis losses and is a source of magnetization energy. This can be schematically described by a slow energy accumulative process that progressively increases the probability of overcoming the potential barrier between one stable energy well to a "deeper" one (see Fig. 8).

The potential wells describe the energy states of adjacent domains magnetization. "State 1" represents the first metastable configuration where the domain wall is pinned by the defect in the lattice and "state 2" describes a more stable energy configuration where the domain is free to shift. In order to move from state 1 to state 2, the domain wall must gain energy A and when the domain shifts to state 2, it will release energy B in a *DC* jump. Hopping from one state to the other would be responsible for the macroscopic *Barkhausen effect*.

We now estimate, based on a simple reasonable physical model, the typical time scale necessary to overcome the potential barrier. This time scale will be evaluated as the ratio between the available power P and the activation energy

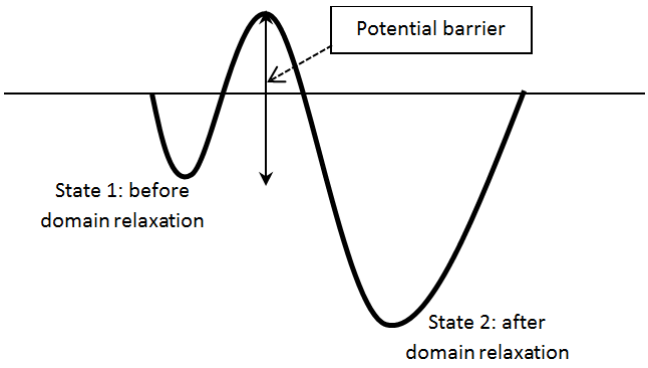

Fig. 8. Schematic view of the energy states and potential describing the DC jump phenomenon.

barrier for the domain unpinning E_b. The main available source of energy comes from iron-loss hysteresis process. According to the Steinmetz equation [36], the volumetric iron-loss power can be written as:

$$P_{iloss} = k_h f B^b_{max}, \tag{4}$$

where f is the excitation frequency, B_{max} is the maximum induction field, and k_h is the Steinmetz hysteresis coefficient that depends on the material properties as well as the exponent b the value of which lies between 2 and 3. Units of P_{iloss} are (W/m^3).

The energy barrier for the domain unpinning comes from the switching field H_s. The volumetric energy E_b is related to H_s by the formula:

$$E_b = \frac{B^2}{2\mu_0} = \frac{1}{2}\mu^2_{wire}\mu_0 H^2_s, \tag{5}$$

Therefore, the units of E_b are (J/m^3). The typical time for overcoming t_{over} the barrier will then be given by the condition:

$$t_{over} \cdot P_{iloss} \approx E_b, \tag{6}$$

Typical values for our system are listed in the table I.

The switching field value has been estimated for a stress of about 500MPa [37]. Substituting these values in Eq. (6) leads to an estimated of t_{over} of about 30 minutes. Such a time scale is much longer than the usual relaxation time in common dissipative process. Moreover, we see that it is in good agreement with our experimental measurements (Fig. 5 and Fig. 6)

B. Dynamics of Multiple Jumps in a Sensor

The observed decreasing rate of the jumps measurements (Fig. 5 and Fig. 6) is due to the distribution of "inhibition seeds" in relation to the location of the magnetization boundary layer in the core. We validate the model in both orthogonal and parallel fluxgates which differ in their magnetization gradient across the core.

One of the cores' inhomogeneity source is the wire drawing production process [38]. The drawing process imprint the core with intrinsic stress field which is typically up to 150 MPa in the inner core and increases exponentially to ~900 MPa in the periphery of the wire [29]. The stress affects the magnetic field

TABLE I
TYPICAL VALUES FOR CO-BASED AMPRPOUS WIRE

	k_h	f	B_{max}	b	μ_{wire}	H_s
Units	J/m^3	kHz	T			A/m
Value	0.25	6	0.5	2.5	10^5	10

required for domain magnetization reversal [38]. For example, the reversal magnetization field at stress of 900 MPa is 2-5 times larger than that required at 150 MPa.

Another source of inhomogeneity in the structure of the core are imperfections existing in the core from its rapid casting process. We assume that the outer shell of the wire has the most imperfections per volume unit because it is the surface in contact with the nozzle during the casting process. The imperfections in the rest of the wire bulk may be assumed uniform per unit of volume.

1) In Wire Core Orthogonal Fluxgates: As described earlier, in wire orthogonal fluxgates the magnetic core is excited by driving current through it, creating shells with different magnetization levels. The instable boundary layer between saturated and magnetized shells is where the jumps originate. Domains with "seeds" of rotation impedance are restricted to this boundary shell. Hence, once this layer has turned, no further jumps are expected. As a result, the amount of jumps is small and the occurrence is random and not progressing.

2) In Parallel Fluxgates: In parallel fluxgates, there is no inherent gradient in the magnetization of the core because the core is excited by a solenoid and not by driving current through the core. The dynamics of the *DC* jumps is therefore determined predominantly by the distribution of the inhibition sources in the core material and the distribution of stress imprinted into the core during casting. We have stated that the wire core drawing process imprints the core with intrinsic stress field. We describe how these facts can explain the long term behavior of *DC* jumps we have seen in Fig. 7.

It has been shown experimentally in [37] how stress applied to the wire affects the field that is required to switch the domain magnetization. Such dependence is also shown in [29] together with the change of the stress value as a function of the distance from the core center. The combination of these two effects can be done according to the following steps:

We first express the internal axial component of the stress as a positive function of the distance from the wire center for the case of as cast wire. Note in Fig. 9 that at half the radius the stress derivative changes sign. This corresponds to the end of the inner core that consists of a mono-domain cylinder with easy magnetization direction parallel to the wire axis [37]. At this point the stress value is approximately 150 MPa.

Annealing the wire core reduces residual stress and anisotropy to improve magnetic softness. It also induces controlled surface crystallization [29]. However, in our case, the parallel fluxgates were annealed and the orthogonal fluxgates were not annealed, nevertheless, both suffered from *DC* jumps.

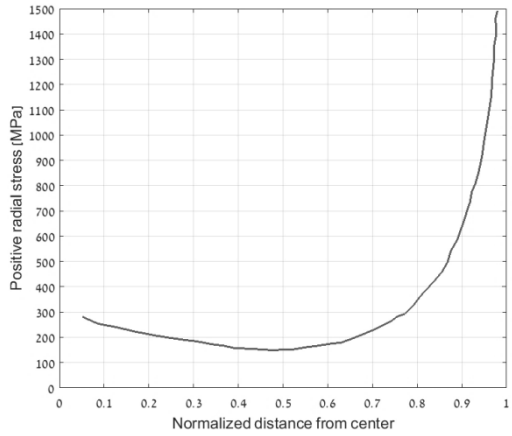

Fig. 9. Internal radial stress as a function of normalized radius of the wire on as cast wire. (from [29, Fig. 7]).

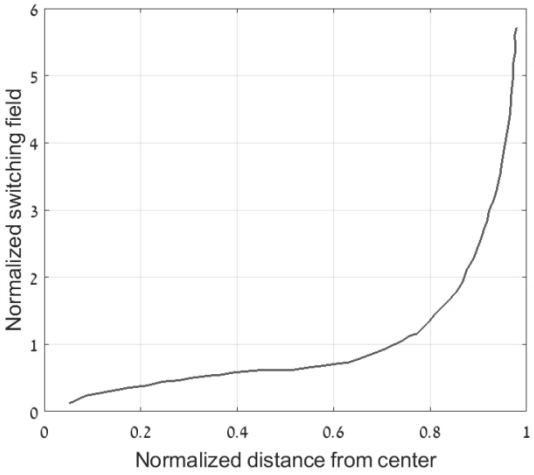

Fig. 10. Normalized switching field as a function of wire radius.

From a simple analysis of the normalized switching field (*NSF*) as a function of the internal stress [29] we produce the normalized switching field as a function of wire radius shown in Fig. 10. We project the switching field into time units in order to determine the dynamics of the jumps subsiding rate. This can be done if one remembers that the *NSF* is proportional to the number of rotation cycles that are required to obtain complete magnetization of a single region. This is also directly related to the switching excitation frequency f_{exc}. Therefore, a simple formula transforms the *NSF* to the time domain:

$$t_{sw} = \frac{C \cdot NSF}{f_{exc}} \cdot SF\,(0)\,, \tag{7}$$

where $SF(0)$ is the switching field value at which the stress is close to 0, and C a constant that depends on physical and mechanical properties of the specific wire.

By using Eq.(7) and Fig. 10, and inverting the X-Y axes one can see the correlation between the radial distance from the wire center to the time required for domain switching. For an example, by using the same parameters as obtained [37] timescale we use excitation frequency of 5 kHz, a zero stress *SF* of 7.5 Am^{-1} [37], and a dimensionless constant C equals to $2.1 \cdot 10^7$. This is shown in Fig. 11.

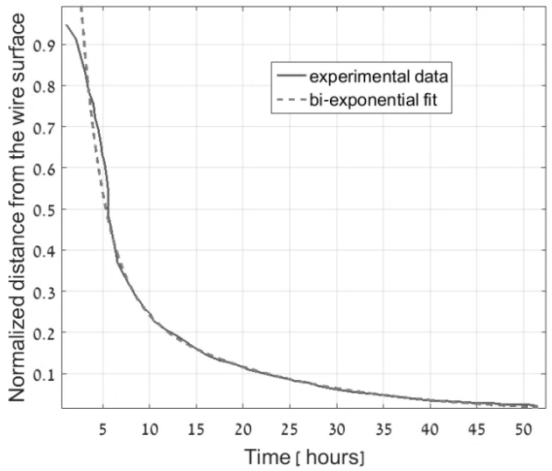

Fig. 11. Switching shells measured from the surface wire (normalized: 1 = surface, 0 = center) as a function of time and Bi-exponential fit used to match the result.

It is not surprising that the best fit for the graph in Fig. 10 also a bi-exponential function, exactly like the fit obtained in our experimental result shown in Fig.11.

V. Discussion

We have presented a straightforward explanation for the bi-exponential behavior we measured. This relation reflects the fact that the large number of jumps at the beginning of the sensor working time has its origin in the inner region of the wire core. This region is probably constituted by a very few number of domains which easily magnetize. This region can be quite large and since it is easily magnetized it produces a large number of jumps right on the onset of the fluxgate operation.

As time progresses, only regions far from the center will provide more jumps. The reason this occurs despite the large internal stress present in this part of the wire, is because, as we increase the radius of these external shells the number of impurities increase as well. These impurities provide excellent starting points for the nucleation process, and it is known that such a nucleation process is necessary to switch the magnetization of a domain into its opposite direction, i.e. to produce a jump.

VI. Conclusion

Large Barkhausen jumps are a common phenomenon in low power fluxgates. While not significantly affecting the noise figure, it does seriously affect the signal fidelity and as a result the magnetometer functionality. The issue of magnetic *DC* jumps in low power fluxgates has not been addressed yet in the literature. We experimentally investigate the occurrence of *DC* jumps on a large number of two types of fluxgates.

We present a new physical dynamical model based on relaxation of magnetic domains trapped in reverse polarity in metallurgical super-structures in the core. The model is analytically expanded to explain how and why the jump phenomenon subside in time. We attribute the *DC* jumps to imperfections in the magnetic core and to the magnetization process ruing excitation. We present good correlation between the dynamic model and the measured data. We show that in a continuous operation, the jumps rate decays exponentially in time but never completely stops.

The signal quality and fidelity in magnetic measuring systems can be significantly improved by a suitable management of the jumps in both parallel and orthogonal low power fluxgates.

References

[1] P. Ripka, *Magnetic sensors and Magnetometers*, 1st ed. Norwood, MA, USA: Artech House, 2001.
[2] M. Janosek, "Parallel fluxgate magnetometers," in *High Sensitivity Magnetometers*, A. Grosz, M. J. Haji-Sheikh, and S. C. Mukhopadhyay, Eds. Cham, Switzerland: Springer, 2017, pp. 41–61.
[3] M. Butta, "Orthogonal fluxgate magnetometers," in *High Sensitivity Magnetometers*, A. Grosz, M. J. Haji-Sheikh, S. C. Mukhopadhyay, Eds. Cham, Switzerland: Springer, 2017, pp. 63–102.
[4] F. Primdahl, "The fluxgate magnetometer," *Elements*, vol. 12, no. 4, p. 241, 1979.
[5] E. Paperno, "Suppression of magnetic noise in the fundamental-mode orthogonal fluxgate," *Sens. Actuators A, Phys.*, vol. 116, no. 3, pp. 405–409, Oct. 2004.
[6] R. Alimi, N. Geron, E. Weiss, and T. Ram-Cohen, "Ferromagnetic mass localization in check point configuration using a Levenberg Marquardt algorithm," *Sensors*, vol. 9, no. 11, pp. 8852–8862, Nov. 2009.
[7] E. Weiss, A. Grosz, and E. Paperno, "Duty cycle operation of an orthogonal fluxgate," *IEEE Sensors J.*, vol. 15, no. 3, pp. 1977–1981, Mar. 2015.
[8] E. Weiss, E. Paperno, and A. Plotkin, "Orthogonal fluxgate employing discontinuous excitation," *J. Appl. Phys.*, vol. 107, no. 9, p. 09E717, May 2010.
[9] E. Weiss, A. Grosz, S. Amrusi, and E. Paperno, "Orthogonal fluxgate employing digital selective bandpass sampling," *IEEE Trans. Magn.*, vol. 48, no. 11, pp. 4089–4091, Nov. 2012.
[10] E. Delevoye, M. Audoin, M. Beranger, R. Cuchet, R. Hida, and T. Jager, "Microfluxgate sensors for high frequency and low power applications," *Sens. Actuators A, Phys.*, vols. 145–146, nos. 1–2, pp. 271–277, Jul./Aug. 2008.
[11] G. Musmann, Ed., *Fluxgate Magnetometers for Space Research*. Norderstedt, Germany: BoD–Books on Demand, 2010.
[12] V. Korepanov and A. Marusenkov, "Flux-gate magnetometers design peculiarities," *Surv. Geophys.*, vol. 33, no. 5, pp. 1059–1079, Sep. 2012.
[13] E. Weiss, R. Alimi, E. Liverts, and E. Paperno, "Excess magnetic noise in orthogonal fluxgates employing discontinuous excitation," *IEEE Sensors J.*, vol. 14, no. 9, pp. 2743–2748, Aug. 2014.
[14] G. Infante, R. Varga, G. A. Badini-Confalonieri, and M. Vázquez, "Locally induced domain wall damping in a thin magnetic wire," *Appl. Phys. Lett.*, vol. 95, no. 1, p. 012503, Jul. 2009.
[15] S. Ghosh and J.-Y. Lee, "A Lorentz force magnetometer based on a piezoelectric-on-silicon square-extensional mode micromechanical resonator," *Appl. Phys. Lett.*, vol. 110, no. 25, p. 253507, Jun. 2017.
[16] C. Buffa, "Lorentz force magnetometers," in *MEMS Lorentz Force Magnetometers*. Cham, Switzerland: Springer, 2018, pp. 13–29.
[17] R. S. Popovic, *Hall Effect Devices*. Bristol, U.K.: Institute of Physics Publishing, 2004.
[18] D. Izci, C. Dale, N. Keegan, and J. Hedley, "The construction of a Graphene hall effect magnetometer," *IEEE Sensors J.*, vol. 18, no. 23, pp. 9534–9541, Dec. 2018.
[19] V. Mor, A. Grosz, and L. Klein, "Planar Hall effect (PHE) magnetometers," in *High Sensitivity Magnetometers*. Cham, Switzerland: Springer, 2017, pp. 201–224.
[20] A. Sheinker, L. Frumkis, B. Ginzburg, N. Salomonski, and B.-Z. Kaplan, "Magnetic anomaly detection using a three-axis magnetometer," *IEEE Trans. Magn.*, vol. 45, no. 1, pp. 160–167, Jan. 2009.
[21] E. Weiss and R. Alimi, *Low-Power and High-Sensitivity Magnetic Sensors and Systems*. Norwood, MA, USA: Artech House, 2018.
[22] K. Mohri, F. B. Humphrey, K. Kawashima, K. Kimura, and M. Mizutani, "Large Barkhausen and Matteucci effects in FeCoSiB, FeCrSiB, and FeNiSiB amorphous wires," *IEEE Trans. Magn.*, vol. 26, no. 5, pp. 1789–1791, Sep. 1990.
[23] M. Vázquez, "Advanced magnetic microwires," in *Handbook of Magnetism and Advanced Magnetic Materials*. Hoboken, NJ, USA: Wiley, 2007, pp. 1–34.

[24] E. Weiss and R. Alimi, *Low-Power and High-Sensitivity Magnetic Sensors and Systems*. Norwood, MA, USA: Artech House, 2018.
[25] *Mag648 and Mag649 Low Power Three-Axis Magnetic Field Sensors*, Bartington Instrum., Witney, U.K., Jul. 2011.
[26] S. Flohrer *et al.*, "Dynamic magnetization process of nanocrystalline tape wound cores with transverse field-induced anisotropy," *Acta Mater.*, vol. 54, no. 18, pp. 4693–4698, Oct. 2006.
[27] R. M. Bozorth and D. M. Chapin, "Demagnetizing factors of rods," *J. Appl. Phys.*, vol. 13, no. 5, p. 320, Apr. 1942.
[28] S. Liu, "Study on the low power consumption of racetrack fluxgate," *Sens. Actuators A, Phys.*, vols. 130–131, pp. 124–128, Aug. 2006.
[29] P. T. Squire, D. Atkinson, M. R. J. Gibbs, and S. Atalay, "Amorphous wires and their applications," *J. Magn. Magn. Mater.*, vols. 132, nos. 1–3, pp. 10–21, Apr. 1994.
[30] Y. Liu, D. J. Sellmyer, and D. Shindo, *Handbook of Advanced Magnetic Materials: Nanostructural Effects. Characterization and Simulation. Fabrication and Processing. Properties and Applications*, vols. 1–4. Springer, 2008.
[31] I. Sasada and H. Kashima, "Simple design for orthogonal fluxgate magnetometer in fundamental mode," *J. Magn. Soc. Japan*, vol. 33, no. 2, pp. 43–45, 2009.
[32] E. Paperno, E. Weiss, and A. Plotkin, "A tube-core orthogonal fluxgate operated in fundamental mode," *IEEE Trans. Magn.*, vol. 44, no. 11, pp. 4018–4021, Nov. 2008.
[33] J. Pommier, P. Meyer, G. Pánissard, J. Ferré, P. Bruno, and D. Renard, "Magnetization reversal in ultrathin ferromagnetic films with perpendicular anistropy: Domain observations," *Phys. Rev. Lett.*, vol. 65, no. 16, pp. 2054–2057, Oct. 1990.
[34] L. Landau and E. Lifshitz, "On the theory of the dispersion of magnetic permeability in ferromagnetic bodies," *Phys. Z, Sowjetunion*, vol. 8, no. 153, pp. 101–114, Jun. 1935.
[35] A. Visintin, "Modified Landau–Lifshitz equation for ferromagnetism," *Phys. B, Condens. Matter*, vol. 233, no. 4, pp. 365–369, Jun. 1997.
[36] C. P. Steinmetz, "On the law of hysteresis," *Proc. IEEE*, vol. 72, no. 2, pp. 197–221, Feb. 1984.
[37] A. M. Severino, C. Gámez-Polo, P. Marán, and M. Vázquez, "Influence of the sample length on the switching process of magnetostrictive amorphous wire," *J. Magn. Magn. Mater.*, vol. 103, nos. 1–2, pp. 117–125, Jan. 1992.
[38] H. Chiriac, S. Corodeanu, M. Lostun, G. Ababei, and T.-A. Óvári, "Magnetic behavior of rapidly quenched submicron amorphous wires," *J. Appl. Phys.*, vol. 107, no. 9, p. 09A301, 2010.

Eyal Weiss, photograph and biography not available at the time of publication.

Roger Alimi, photograph and biography not available at the time of publication.

Amir Ivry, photograph and biography not available at the time of publication.

Elad Fisher, photograph and biography not available at the time of publication.